OA-Bug: Olfactory-Auditory Augmentation for Swarm Exploration in Denied Environments

Anonymous CVPR submission

Paper ID Non-proceedings Workshop

Abstract

Searching in denied environments remains challenging for embodied robotic systems when vision, GNSS, mapping, and communication infrastructure are unavailable. This work investigates whether non-visual sensory modalities, specifically olfactory and auditory cues, can structure decentralized spatial exploration in such settings. We propose OA-Bug, an olfactory-auditory augmentation of the classical Bug Algorithm that integrates chemical stigmergy for revisitation awareness and signal-based relative localization for spatial dispersion. Rather than relying on global coordination, each robot locally deposits and detects chemical markers and adapts its preferred exploration direction based on neighboring auditory cues, enabling emergent coverage behavior through multi-sensory interaction. Extensive simulations demonstrate that olfactory feedback substantially reduces revisitation, while auditory coordination improves spatial dispersion under constrained deployment conditions. Real-world experiments with physical swarm robots further validate that the proposed multi-sensory mechanism remains effective under sensing uncertainty and environmental irregularities. Our results suggest that non-visual modalities can influence collective spatial behavior in embodied systems, offering a lightweight and infrastructure-free approach to decentralized exploration. Our code will be released.

1. Introduction

Robotic search and rescue (RSAR) holds great promise by reducing risks and operational costs associated with human rescuers while improving response efficiency through multi-robot systems (MRS). A swarm of autonomous robots equipped with onboard sensors can provide rapid situational awareness [18, 26], real-time mapping and accident scene monitoring [12, 14], and crucial support in hazardous environments [19, 28]. Compared with human rescuers, robotic systems can operate in confined, toxic, or structurally unstable environments with reduced safety concerns.

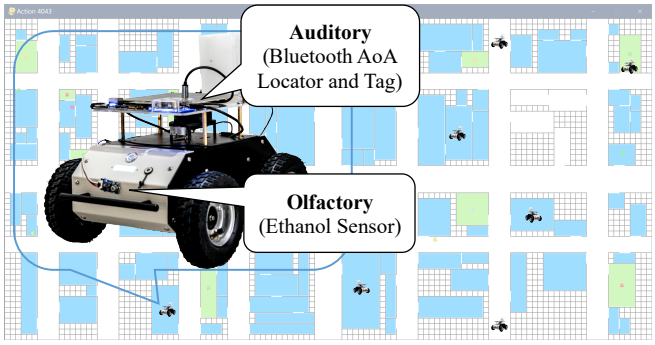

Figure 1. Swarm Robots with Olfactory and Auditory Sensing

While previous researchers have proposed feasible solutions for RSAR to reduce time costs and improve search coverage [8, 9, 17, 27, 31], and others have developed strategies to enhance MRS robustness [4, 30], these approaches heavily rely on external resources or prior knowledge. Typically, robots pre-plan their paths and follow calculated routes aided by the Global Navigation Satellite System (GNSS) or pre-built maps, rather than making decisions based on local environmental perception. However, GNSS signals may be unavailable in disaster scenarios, and the rescue scene is often completely unknown. Furthermore, algorithms requiring centralized processing or continuous data sharing depend on robust network infrastructure, which is highly impractical under poor communication conditions.

We define such settings as *denied environments*: unknown environments where global positioning is unavailable and communication is constrained. Previous research introduced graph-based models for multi-robot coverage in denied environments [32], including the use of RFID tags as coordination points for pose memorization and updates [34]. However, these graph-based approaches require internal memory, are computationally expensive, and scale poorly in large, complex environments [25]. Alternative stigmergic methods, such as robots leaving physical pen-marked trails to cover closed terrains [29], may struggle in dirty or low-light conditions. Other non-graph stigmergic

approaches like MAW [21], StiCo [25], and S-MASA [33] lack hardware implementation. MAW [21] requires finding a new direction with the lowest pheromone level at each step, which is practically time-consuming. StiCo [25] and S-MASA [33] remain unvalidated in complex structural layouts (e.g., nested rooms) where robots might redundantly attempt to fully cover a space, leading to entrapment. Moreover, existing methods rarely address inter-robot coordination during simultaneous departure, nor do they exploit relative positions to guide subsequent decisions.

The classical Bug Algorithm is a lightweight motion-planning algorithm that requires only local sensing and a goal direction [13]. Due to its simplicity and minimal resource requirements, it is attractive for hardware implementation. While numerous variants exist [16], including vision-based adaptations that utilize SIFT [3] or Bag-of-Words [2] for scene feature memorization, these demand extra memory and may degrade in poor lighting where textures are unrecognizable. SGBA [17] offers a swarm exploration solution for denied environments; however, it relies on a centralized Wi-Fi home beacon to provide global reference information, limiting applicability in infrastructure-free scenarios due to power dependency, deployment challenges, interference, or signal shielding.

In denied environments, biological systems—both humans and animals—excel at acquiring and transmitting spatial information through olfaction and audition. Rescuers in caves call out to infer relative positions; forest-dwelling animals communicate through chirps when visual line-of-sight is blocked; ants release chemical pheromones that persist in space, utilizing a "hysteresis effect" for trail marking. These observations motivate the question: *can olfactory and auditory cues be integrated into the Bug Algorithm for decentralized swarm exploration, and validated on real robots?*

To implement this bio-inspired, multi-sensory modeling in hardware, practical engineering proxies can be integrated for olfaction and audition. For olfaction, low-cost gas sensors have been successfully deployed to track chemical gradients in diffusive environments [10], and robotic systems have even incorporated biological insect antennae for odor sensing [1, 11, 15, 20], suggesting that odor-based spatial memory is feasible. For audition, ODAS [6, 7] is a well-established framework for sound source localization (SSL) and tracking, optimized for accurate, fast, and robust performance. However, in our initial deployments, acoustic-based localization proved susceptible to environmental acoustic interference and was limited in transmission range. To overcome these physical limitations while strictly preserving the bio-inspired paradigm of local, directional broadcasting, we utilize the Bluetooth 5.1 Direction Finding standard [22]. This RF-based approach provides higher precision, extended range, and more robust source localization and tracking capabilities, effectively serving as the "auditory" modality that allows the swarm to establish a decentralized spatial awareness.

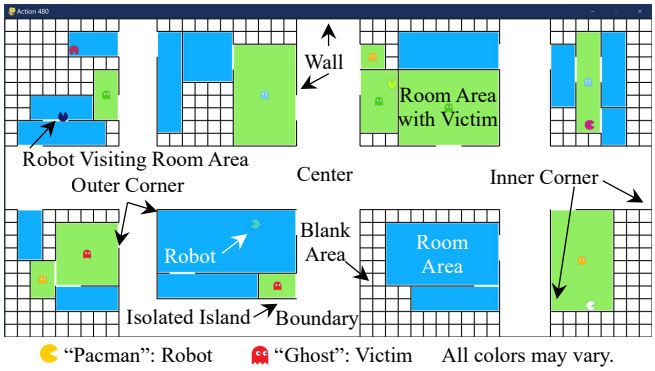

Figure 2. Site Definitions and Geometric Descriptions

In this paper, we propose OA-Bug, an Olfactory-Auditory Augmented Swarm Bug Algorithm for decentralized exploration in denied environments. Each robot deposits a detectable scent (e.g., ethanol) along its trajectory to mark visited regions, enabling indirect coordination through environmental memory. When encountering such markers, robots use signal-based relative localization to infer the relative positions of their peers and adjust their motion accordingly. The method requires no GNSS, mapping, data sharing, or centralized processing.

Our contributions are as follows:

- A bio-inspired augmentation of the lightweight Bug Algorithm that integrates olfactory stigmergy and auditory relative localization for decentralized swarm exploration.
- A hardware-implementable framework that avoids centralized infrastructure and heavy memory requirements.
- Validation in both simulation and real-world swarm experiments, demonstrating improved coverage efficiency in denied environments.

Rapid victim localization is critical in disaster response, where survival probability decreases with rescue delay [5]. By improving decentralized exploration efficiency under severe environmental constraints, OA-Bug provides a practical step toward more resilient robotic search systems.

2. Method

2.1. Problem Statement

Consider a search scenario taking place within a static, 2D planar site S composed of walls $\{w_i\}_{i=1}^{n}$ $(n > 1)$, room areas $\{a_i\}_{i=1}^{m}$ $(m > 1)$, and a set of non-visitable blank areas B. A swarm of robots is denoted by $R = \{r_i\}_{i=1}^{p}$ $(p > 1)$, and optional static victims by $V = \{v_i\}_{i=1}^{q}$ $(0 \leq q \leq p)$. These symbols serve as identifiers only for notational convenience.

The site has two key properties:

1) Unfamiliarity: the environment is unknown a priori. No GNSS, global map, or communication infrastructure is available.

2) Closure: the site is enclosed by walls that robots cannot traverse or destroy, and has a single entrance/exit for robot deployment.

We define the projection of a *wall* onto the site as a continuous curve with two *endpoints*. A *room* is defined as a union of walls. The projection of a room onto the site forms a planar figure with at least one opening (i.e., at least two endpoints). The total number of endpoints is assumed to be even, such that the endpoints can be paired to form a minimally enclosed region. This enclosed region is defined as a *room area*. An *isolated island* is defined as a set of interconnected rooms whose walls do not connect to the outer boundary of the site. For simplicity and realism, we assume that walls are straight line segments. At the intersection of two walls, the smaller interior angle is defined as an *inner corner* and the larger angle as an *outer corner*. Some of these definitions are illustrated in Fig. 2.

All robots are identical, sharing the same action space $\mathcal{A} = \{\text{go straight}, \text{turn}\}$, state space, and sensing capabilities. Robots are deployed from a designated origin (e.g., the site *center* or *boundary*). Their task is *cooperative spatial exploration*: navigating and searching as many unvisited room areas as possible within a given timeframe to locate victims (if any), but no specific goal is assigned to individual robots. During this task, robots cannot memorize or share their exact states. Without augmentation, a robot can only detect collisions with walls or other robots, whether it is at an outer corner, and whether it has found a victim.

To facilitate multi-sensory spatial awareness under these strict constraints, each robot is equipped with the following four sensor modalities:

1) Ranging Sensor: Detects physical boundaries like walls, robots, and victims within sensing range. It returns relative positions with respect to the local frame of the source robot.

2) Olfactory Sensor: Measures accumulated chemical markers. It returns the number of times the current location $l_{ci} \in S$ has been visited by the swarm.

3) Auditory Sensor: Enables local peer-to-peer relative positioning. It returns $\boldsymbol{p}_j = (\rho_j, \theta_j)$ for any other robot r_j ($j \neq i$) within range, where ρ_j is relative distance and θ_j is relative azimuth with respect to the source robot r_i.

4) Orientation Sensor: Allows the robot to maintain or turn toward a desired azimuth. It returns the robot's current heading, functioning as a local compass.

To isolate algorithm design from hardware-specific noise, we adhere to the classical Bug Algorithm assumption of utilizing idealized, deterministic sensors that do not involve probabilistic uncertainties.

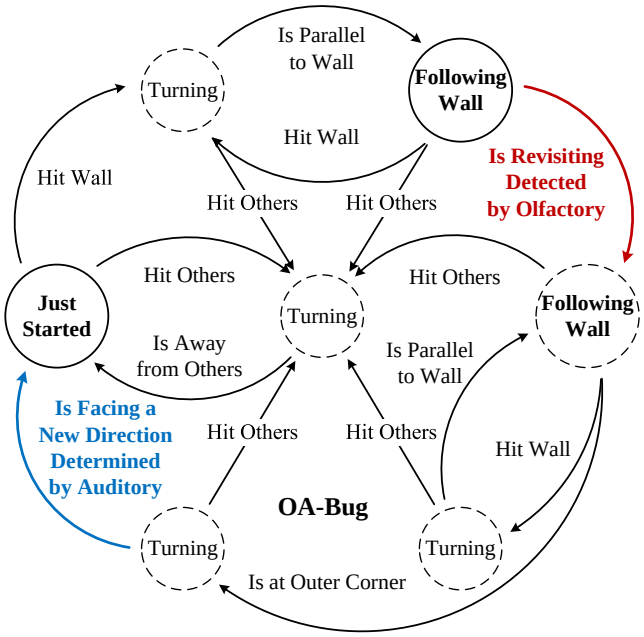

Figure 3. Finite State Machine of the OA-Bug Algorithm

2.2. Algorithm Formulation

The design of OA-Bug follows three principles:

1) Revisitation Minimization: Previously explored regions should not be repeatedly visited.

2) Dispersion Promotion: Robots should maintain spatial separation to reduce clustering.

3) Coverage Continuity Maximization: If an area has not yet been explored, the robot should continue searching it rather than prematurely changing direction.

To augment the classical Bug Algorithm, we incorporate olfactory stigmergy and auditory relative localization. While moving, each robot continuously broadcasts signals to indicate its relative position and deposits a detectable chemical marker to mark its trajectory as visited space. Thus, olfaction allows the robot to detect whether the current location $l_{ci} \in S$ has been visited, and audition provides information about others' relative positions to choose a better turning direction φ_i when it hits a wall or revisits a place.

Preferred Direction Initialization. Unlike classical Bug algorithms that pursue a fixed target, OA-Bug assigns each robot a *preferred direction* φ_i. This reflects realistic rescue scenarios where victim locations are unknown. Specifically, if n robots are deployed simultaneously from a common origin, the preferred direction φ_i for the i-th robot (out of n total robots) can be initialized as

$$\varphi_i = \frac{\alpha i}{n} + \text{bias}, \tag{1}$$

where the bias is an arbitrary angular offset identical for the entire deployment group, and $\alpha \in (0, 2\pi]$ is the angu-

Table 1. Comparison of Ablation Baseline and OA-Bug Variants

Algorithm	Explanation	From Just Started to Following Wall	In Following Wall and at Outer Corner
Random	Blank Control	turns at a random angle	moves forward or turns randomly
Minimum	"Bug 0"-Like Variant	turns in a uniform direction (e.g., right)	turns toward φ_i
Auditory Only	w/ Direction Update	updates φ_i' and turns to align with the wall	updates φ_i' and turns toward it
Olfactory Only	"Bug 1" w/ Revisitation Feedback	turns in a fixed direction	if revisitation is detected, turns toward φ_i (reversed if visited ≥ 3 times); otherwise continues wall following
Olfactory + Auditory	Full OA-Bug	updates φ_i' and turns to align with the wall	if revisitation is detected, turns toward updated φ_i' (reversed if visited ≥ 3 times); otherwise continues wall following

lar span of the initial heading sector. Under unconstrained deployment (e.g., from the site center), $\alpha = 2\pi$ distributes headings uniformly over the full circle. Under geometrically constrained deployment, α and bias can be reduced so that initial headings are distributed within a narrower sector, reflecting the limited angular freedom available at the site.

Auditory-Based Direction Update. The auditory output $\boldsymbol{p}_j$ is converted to Cartesian vectors $\boldsymbol{c}_j = (\Delta x_j, \Delta y_j)$, where $\rho_j^2 = \Delta x_j^2 + \Delta y_j^2$ and $\tan\theta_j = \frac{\Delta y_j}{\Delta x_j}$ for $\Delta x_j \neq 0$. To encourage dispersion, the robot computes the opposite direction vector

$$\boldsymbol{c}_{i,\text{opp}} = -\sum_j \boldsymbol{c}_j, \tag{2}$$

which is then converted back to polar coordinates $\boldsymbol{p}_{i,\text{opp}} = (\rho_{i,\text{opp}}, \theta_{i,\text{opp}})$, establishing the new preferred spatial heading $\varphi_i' = \theta_{i,\text{opp}}$. This update is applied when the robot needs to re-orient after collisions or revisiting.

Finite-State Control. The logic is modeled as a finite state machine (FSM), shown in Fig. 3, with two primary states:

1) Just Started: The robot is either at the beginning of its search or has just changed direction after encountering another robot or revisiting a location.

2) Following Wall: The robot has just encountered a wall and is following it to explore adjacent room areas.

The state transition triggers are as follows:

1) Hitting Wall: When a robot in the Just Started state encounters a wall, it transitions to Following Wall. If already in Following Wall, it maintains this state.

2) Hitting Others: When a collision with another robot occurs during Following Wall, the robot transitions back to Just Started. If the robot is in the Just Started state, it remains in that state. All robots then turn in a consistent direction to reduce repeated collisions and revisits.

3) At Outer Corner: If the robot is in the Following Wall state and detects that the current location has already been visited, it transitions to Just Started. If the robot enters the Just Started state due to revisiting, it changes its orientation.

Procedural Description. More specifically, each robot initializes its state to Just Started and moves in its preferred direction φ_i until it encounters a wall. It then transitions to Following Wall and proceeds along the wall boundary. If it detects the entrance to a room area, it enters and continues moving along the room boundary. When one room leads to another, the robot first searches along the inner wall of the connected room and then along the outer wall, similar to a depth-first search behavior. This approach enables the robot to explore as many room areas as possible, thereby increasing coverage.

If the robot detects a scent at an outer corner of the wall, this indicates that the area has already been visited, and the robot schedules a φ_i update. It continues following the wall until it reaches the next outer corner, where it updates its direction to φ_i' and may leave the wall, transitioning back to the Just Started state.

The preferred direction φ_i is primarily updated using auditory information. However, if the robot detects that a location has been visited multiple times (e.g., three times, as inferred via olfaction), it assumes that the nearby area has been sufficiently explored and sets its new direction to $\varphi_i' + \pi$, i.e., opposite to its previous preferred direction. Ideally, this causes the robot to explore a region symmetric with respect to the departure point, thereby reducing overlap with previously explored areas.

2.3. Mechanism Insight

OA-Bug can be viewed as a distributed coverage mechanism arising from the interaction of two components: stigmergic spatial memory and distributed repulsive interaction.

Olfactory Feedback as Stigmergic Spatial Memory. Unlike explicit mapping, olfaction creates a spatial memory field embedded in the environment itself, enabling robots to avoid repeated traversal without storing global state. As chemical markers accumulate in explored regions, revisitation detections increase and trigger direction changes. This can be interpreted as a stigmergic inhibition mechanism that progressively pushes robots away from saturated areas.

Auditory Coordination as Distributed Repulsive Interaction. Spatial dispersion arises from two complementary mechanisms. First, preferred directions are initialized to be evenly spaced at deployment, preventing heading alignment that would otherwise cause robots to follow identical or colliding trajectories. Second, during exploration, audition up-

dates Eq. 2, adjusting each robot's preferred direction opposite to the aggregated relative positions of its peers. This update can be interpreted as approximating a distributed repulsive potential field, encouraging robots to spread out without explicit communication or global coordination.

Emergent Coverage Behavior. Together, these mechanisms form a decentralized exploration process. Olfactory feedback prevents revisitation by penalizing saturated regions, while auditory coordination reduces clustering and improves spatial spread. Although no explicit global coverage objective is encoded, their interaction produces emergent coverage-oriented behavior under severe sensing and communication constraints.

3. Software Simulation

3.1. Evaluation Hypotheses

Based on the mechanism analysis in the previous section, we formulate the following hypotheses regarding OA-Bug:

H1: Olfactory feedback is the primary contributing factor in coverage improvement. By introducing the stigmergic spatial memory, olfactory sensing should significantly reduce revisitation and increase overall coverage compared to algorithms without such feedback.

H2: Auditory coordination primarily improves dispersion under constrained deployment conditions. When robots are deployed from spatially restricted positions (e.g., boundary deployment), auditory-based repulsion should improve spatial spreading and reduce clustering effects.

H3: Increasing robot count improves coverage with diminishing returns. Due to spatial interference and overlapping exploration regions, marginal gains in coverage are expected to decrease as swarm size increases.

The simulation study is designed to evaluate these hypotheses through comparisons between OA-Bug and ablated variants of our approach under varying environment scales and deployment configurations.

3.2. Simulation Environment

To gain full control over the simulation process, we built the environment almost entirely from scratch. It consists of three main components:

1) Site Generator: Generates random but valid site layouts that conform to the definitions in Sec 2.1. Layout parameters (dimensions, number of rooms, corridor widths, number of victims) are configurable, enabling large-scale evaluation while avoiding bias introduced by handcrafted environments.

2) Layout Module: Parses the generated or manually defined site data and instantiates the environmental objects. When graphics mode is enabled, it renders the 2D spatial layout, as illustrated in Fig. 1 and Fig. 2.

Table 2. Simulation Site Configurations

Configuration	Width ($\times\frac{4}{15}$m)	Height ($\times\frac{4}{15}$m)	Area (m^2)	# of Rooms	Max Actions Per Robot*
Large	120	60	512	120	4000
Medium	80	40	228	60	2000
Small	60	30	128	30	1000

*Units and values are selected to reflect realistic site scales while remaining suitable for visualization.

3) Robot Module: Handles the instantiation and execution of the swarm agents under a unified interface, applying the specific algorithms under test. Although the underlying engine maintains absolute global coordinates for rendering purposes, the agents have no access to a global map and do not use absolute position information for decision-making.

3.3. Simulation Design

We compare five algorithm variants (Table 1) under three site scales (Table 2). For each configuration, 100 independent site layouts were generated, 2, 4, 6, 8, and 10 robots were deployed, and robots departed from either the center or the boundary. Metrics recorded every 100 actions include total coverage, per-robot coverage, and collision count. A room is considered "covered" once a robot enters its defined area. Each run terminates when all rooms are covered or when robots exhaust the maximum action limit.

For challenging boundary deployment, we restrict the initial preferred directions to span only a π sector (i.e., $\alpha = \pi$ in Eq. 1) while leaving the bias term unrestricted. Since the shared bias is not controlled, the entire heading sector may be oriented toward the boundary, modeling unfavorable deployment conditions such as launch misalignment or heading drift. Importantly, the same initialization protocol is applied to all algorithm variants to ensure fair comparison, and all results are averaged over randomized biases and site instances.

3.4. Simulation Results and Discussion

Our analysis focuses primarily on *room visitation coverage*, defined as the fraction of unique rooms entered at least once, as it is the critical metric for successful spatial exploration. The aggregated results, presented in Fig. 4, indicate that OA-Bug consistently achieves high coverage in denied environments, reaching up to 96.93%. As no dedicated victim-handling mechanisms were designed, victim-related analysis is reserved for future work.

Effect of Olfactory Feedback. Algorithms incorporating olfactory feedback significantly outperform other baselines across all configurations. In particular, under the Large configuration, the coverage of Minimum and Auditory Only is nearly as low as that of the Random baseline. This confirms that revisitation awareness enabled by the stigmergic spatial memory is the primary factor improving coverage,

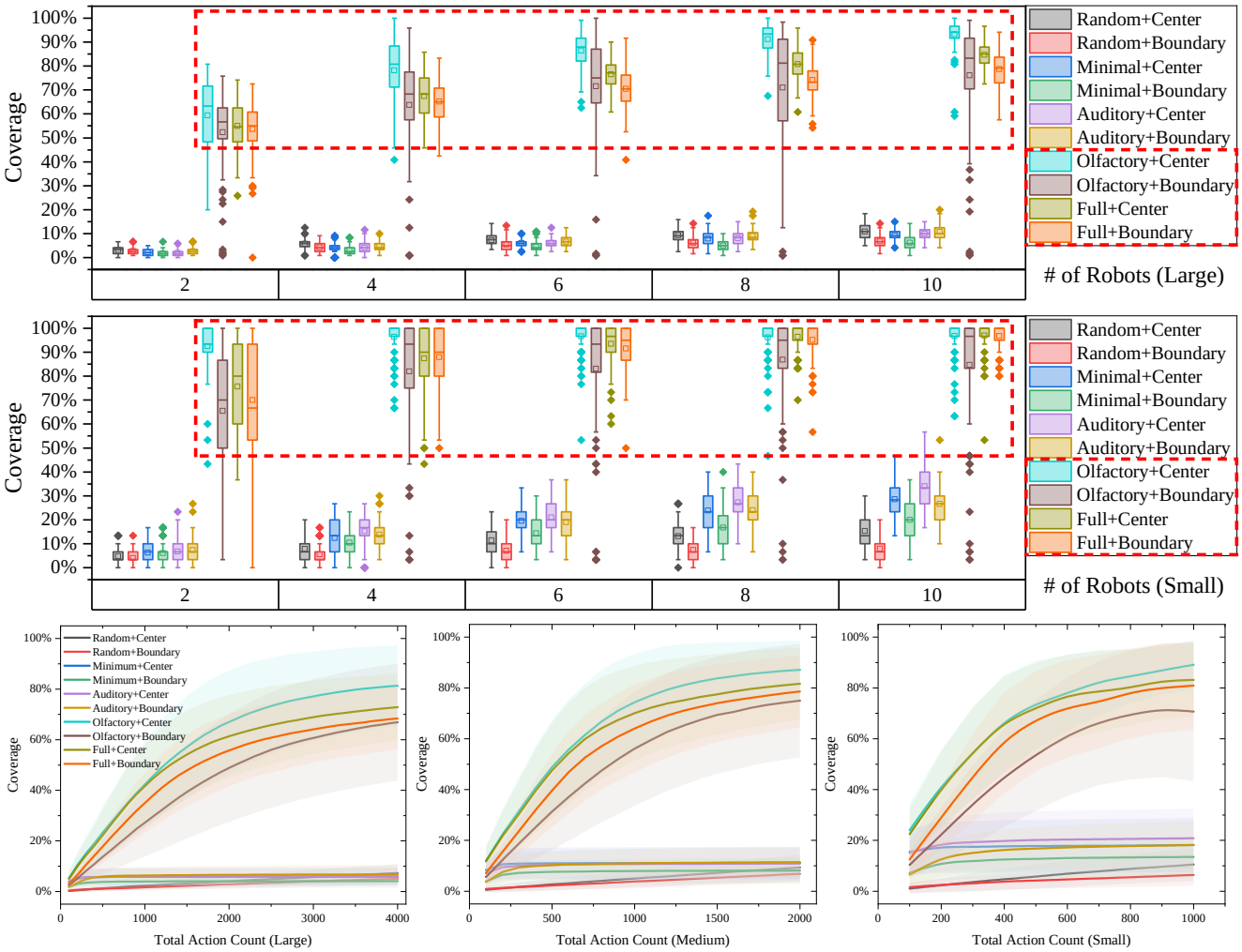

Figure 4. Simulation Coverage Results. Average coverage relative to total action count appears lower than actual coverage, as trials achieving 100% coverage terminate early, halting further action logging. The remaining lower-coverage portion reflects more challenging scenarios in which full coverage is harder to achieve.

suggesting that such awareness and its corresponding direction changes are critical in large, complex environments.

Effect of Robot Count. Coverage increases with the number of robots, while the standard deviation decreases. However, marginal gains diminish as robot count grows, especially in Small and Medium configurations. This suggests that in real-world deployments, swarm size should be carefully optimized relative to the estimated scale of the search space to ensure resource efficiency.

Effect of Deployment Position. Deployment from the center generally yields higher coverage with fewer actions than deployment from the boundary, as the swarm can immediately disperse radially. However, real-world scenarios often constrain deployment to boundary locations, making boundary performance particularly important.

Role of Auditory Coordination. When robots depart from the center, Olfactory Only achieves higher coverage than OA-Bug. In contrast, under boundary deployment, OA-Bug outperforms Olfactory Only in challenging scenarios. In the Small configuration, the boundary-departure coverage of OA-Bug is higher than that of Olfactory Only and is nearly comparable to its center-departure performance. Moreover, to reach the same coverage level under boundary deployment, OA-Bug requires fewer actions than Olfactory Only. These differences can be attributed to the contribution of auditory-based coordination.

When robots depart from the center, sufficient space allows for natural dispersion. Here, it is advantageous for all robots to turn in the same direction (e.g., uniformly turning right) upon first encountering a wall. This produces a coherent clockwise or counterclockwise exploration pattern that reduces collisions. Since Olfactory Only follows this strategy, it achieves higher coverage under center deployment.

In contrast, when robots depart from the boundary, the

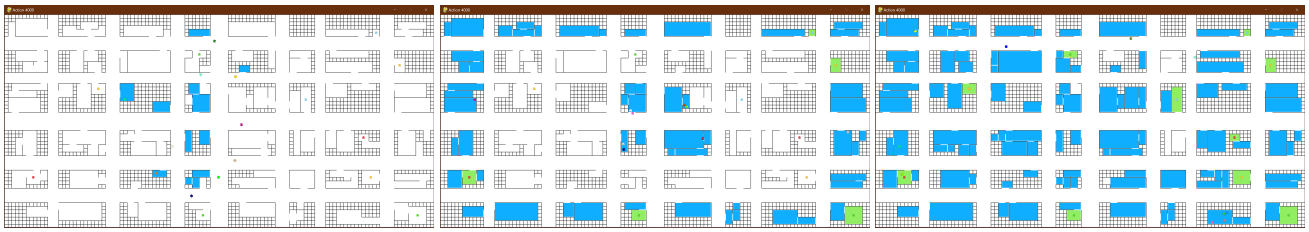

(a) Random Baseline (b) Illustrative Coverage of SGBA [17] (c) Representative Best Result of OA-Bug

Figure 5. Sample Visualization of Search Coverage across Algorithms. The schematic illustration of SGBA [17] is based on the FSM described in the original paper and adapted to our environmental constraints.

initial space is constrained. Here, it is more beneficial for robots to turn in different directions to promote spatial spreading and reduce revisitation. OA-Bug achieves this behavior through auditory-based direction updates, leading to higher coverage under boundary deployment.

In essence, auditory-based direction updates equip the multi-robot system with a distributed repulsion effect, which is especially valuable when natural geometric conditions fail to guarantee adequate dispersion.

Comparison with SGBA [17]. Despite the assistance of the Wi-Fi home beacon and the center deployment strategy in SGBA [17], OA-Bug achieves higher coverage. Since their experimental environment is smaller and less complex, directly porting SGBA to our platform may lead to degraded performance. While a full re-implementation of SGBA under identical simulation settings remains future work, Fig. 5 illustrates the enhanced emergent coverage pattern of our decentralized, multi-sensory approach.

4. Real-World Experimental Results

To validate OA-Bug on hardware and assess whether real-world behavior is consistent with simulation, we implemented the full system on physical robots and conducted on-site experiments.

4.1. Hardware Setup

Four identical robots were deployed. Each robot (Fig. 1) was equipped with a Raspberry Pi 4B onboard controller, an MP503 ethanol sensor for olfactory sensing, a Silicon Labs BG22-RB4191A Bluetooth 5.1 antenna array radio board as its auditory locator, a Silicon Labs SLTB010A EFR32BG22 Thunderboard Kit as its sound tag, a Slamtec RPLidar A1 for wall following and obstacle detection, an MPU6050 IMU for direction control, and a 3D-printed ethanol tank with a 3-watt pump for volatile chemical marking.

Auditory Localization. Each tag has a unique MAC address and transmits signals using the Bluetooth 5.1 protocol, which can be received by every auditory locator within range. The received signals are processed using the angle-of-arrival (AoA) algorithm implemented in the Gecko library. The relative direction of the tag with respect to the locator can then be estimated in real time with an error of less than 5°[1]. Each robot ignores signals from its own tag.

Although Bluetooth signals are used to emulate audible sound, no state information is shared between robots. Our implementation leverages the Bluetooth 5.1 Direction Finding standard, which provides sub-meter positioning accuracy, a significantly longer operational range (approximately 30–50 m under 4 to 0 wall obstructions, as tested by us), and more robust source localization and tracking performance than acoustic-based approaches [22].

Olfactory Marking. The placement of the gas sensor and ethanol tank is carefully designed to prevent the robot's released ethanol from interfering with its own sensor readings. The pump releases 75% ethanol every 5 s for 0.5 s. The gas sensor's analog output is sampled by a 10-bit ADC, yielding values in the range of 0–1023. Under normal conditions, the digital reading is typically below 100. When the sensor passes within approximately 1 m of recently released ethanol (as described above), the reading generally exceeds 100 within 5 s and then falls below 200 within 10 s. We therefore set 200 as the threshold to determine whether a location has been revisited. Experiments were conducted in an indoor environment with closed windows and mild air conditioning, maintaining a temperature of approximately 27 °C and minimal air turbulence. These parameters may vary under different environmental conditions.

Wall Following and Obstacle Avoidance. Although equipped with LiDAR, robots do not build maps. For wall following, raw scans are first filtered to remove outlier points, after which line segments are extracted using a split-and-merge procedure and refined via weighted least-squares line fitting to estimate line parameters and their associated covariance matrices [23]. For obstacle avoidance, LiDAR returns are geometrically clustered to detect obstacles and trigger local avoidance behaviors [24].

4.2. Experimental Design

Experiments were conducted in a complex indoor site containing at least one isolated island (see Sec. 2.1). In isolated

[1] As officially claimed and demonstrated by Silicon Labs: https://youtu.be/c3XqbEKmNcM, last visited on 2026-3-2.

island scenarios, robots without global coordination may repeatedly circulate within local loops. This ensures that both olfaction and audition are necessary for high coverage by redirecting robots away from saturated regions.

To isolate the evaluation of the macro-level spatial exploration strategy from micro-level clutter navigation, physical room interiors (which contained dense, irregular furniture) were bypassed via closed doors. Because entering and exiting a room geometrically equates to continuous wall-following under our FSM logic, a robot successfully navigating the exterior perimeter of a room was recorded as having "covered" that specific spatial zone.

Deploying from a constrained boundary location with their initialized preferred direction, the swarm operated autonomously under human observation. Trials were terminated when the site was thoroughly explored or after 20 minutes had elapsed.

4.3. Experimental Results and Discussion

Across six valid trials, robots covered an average of 15.17 out of 18 rooms, corresponding to 84.26% coverage. This coverage exceeds that reported for SGBA [17], although their real-world environment did not include any isolated islands. The best-performing trial is illustrated in Fig. 6.

Consistency with Simulation. Although real-world coverage is lower than simulation results, the overall performance trends remain consistent: the robots avoid becoming trapped in narrow corridors and reduce repeated visits to previously explored locations, demonstrating the effectiveness of OA-Bug.

Robustness Under Real-World Conditions. The algorithm was derived under ideal sensing assumptions to isolate its core behavioral mechanism. In practice, sensing is affected by gas diffusion variability, angular estimation error in Bluetooth AoA, and irregular wall geometries.

Despite these non-ideal factors, OA-Bug maintains high coverage performance. This indicates that the algorithm relies primarily on qualitative directional cues rather than precise measurements: olfactory sensing only needs to coarsely indicate revisitation, and auditory localization only needs to approximate peer direction. As a result, the negative spatial memory and distributed repulsion remain effective under moderate sensing uncertainty.

Factors Limiting Coverage. The lower coverage observed in real-world experiments compared to simulations can be attributed to several factors. First, real-world walls are not always perfectly flat or straight, causing portions of the walls to be detected as obstacles. Nevertheless, the achieved coverage remains acceptable, even though our wall-following and obstacle-avoidance implementation does not rely on computationally intensive approaches such as machine learning. Second, some robots experienced hardware failures during certain trials. Despite this, the remaining functional robots continued to contribute to overall coverage, demonstrating the algorithm's robustness to partial hardware failure.

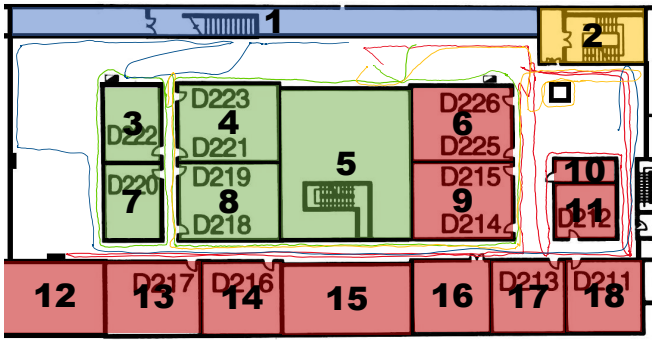

Figure 6. Representative Real-World Trial. Rooms are numbered, and paths are color-coded by robot. The color of a room indicates the robot that first visited it.

5. Conclusion and Future Work

This paper investigates whether non-visual sensory modalities can structure decentralized spatial exploration in robotic systems. We presented OA-Bug, an olfactory-auditory augmentation of the classical Bug Algorithm that integrates chemical stigmergy and signal-based relative localization to enable emergent coverage behavior without GNSS, global mapping, centralized processing, and data sharing.

Through extensive simulations and real-world experiments, we demonstrated that multi-sensory interaction can significantly reduce revisitation and improve spatial dispersion under severe environmental constraints. More broadly, the results indicate that even low-resolution non-visual cues can influence collective spatial behavior, suggesting that multi-sensory interaction provides a viable mechanism for decentralized exploration in embodied robotic systems.

In future work, OA-Bug could be extended to support additional tasks beyond exploration, such as returning to the departure point after mission completion, navigating back when a robot's battery is low, or responding to external summons. From a theoretical perspective, macro-level modeling of swarm dynamics could provide analytical insights into convergence properties and scalability. Furthermore, incorporating more realistic sensor uncertainty models and extending the framework to aerial robotic platforms would enable the transition from 2D planar coverage to 3D spatial exploration, and help connect decentralized control with multi-sensory spatial modeling for embodied intelligence.

References

[1] Melanie J Anderson, Joseph G Sullivan, Timothy K Horiuchi, Sawyer B Fuller, and Thomas L Daniel. A bio-hybrid

odor-guided autonomous palm-sized air vehicle. *Bioinspiration & Biomimetics*, 16(2):026002, 2020. 2

[2] Friedrich Fraundorfer, Christopher Engels, and David Nistér. Topological mapping, localization and navigation using image collections. In *2007 IEEE/RSJ International Conference on Intelligent Robots and Systems*, pages 3872–3877, 2007. 2

[3] Toon Goedemé, Marnix Nuttin, Tinne Tuytelaars, and Luc Van Gool. Omnidirectional vision based topological navigation. *International Journal of Computer Vision*, 74(3): 219–236, 2007. 2

[4] Puneet Goel, Stergios I. Roumeliotis, and Gaurav S. Sukhatme. Robust localization using relative and absolute position estimates. In *1999 IEEE/RSJ International Conference on Intelligent Robots and Systems*, pages 1134–1140, 1999. 1

[5] Siobhan Grayson. Search & rescue using multi-robot systems. *School of Computer Science, University College Dublin*, 2014. 2

[6] François Grondin and François Michaud. Lightweight and optimized sound source localization and tracking methods for open and closed microphone array configurations. *Robotics and Autonomous Systems*, 113:63–80, 2019. 2

[7] François Grondin, Dominic Létourneau, Cédric Godin, Jean-Samuel Lauzon, Jonathan Vincent, Simon Michaud, Samuel Faucher, and François Michaud. ODAS: Open embedded audition system. *Frontiers in Robotics and AI*, 9:854444, 2022. 2

[8] Sabine Hauert, Severin Leven, Maja Varga, Fabio Ruini, Angelo Cangelosi, Jean-Christophe Zufferey, and Dario Floreano. Reynolds flocking in reality with fixed-wing robots: Communication range vs. maximum turning rate. In *2011 IEEE/RSJ International Conference on Intelligent Robots and Systems*, pages 5015–5020, 2011. 1

[9] James M. Hereford. Analysis of a new swarm search algorithm based on trophallaxis. In *IEEE Congress on Evolutionary Computation*, pages 1–8, 2010. 1

[10] Michael Hutchinson, Cunjia Liu, and Wen-Hua Chen. Information-based search for an atmospheric release using a mobile robot: Algorithm and experiments. *IEEE Transactions on Control Systems Technology*, 27(6):2388–2402, 2018. 2

[11] Yoshihiko Kuwana, Sumito Nagasawa, Isao Shimoyama, and Ryohei Kanzaki. Synthesis of the pheromone-oriented behaviour of silkworm moths by a mobile robot with moth antennae as pheromone sensors. *Biosensors and Bioelectronics*, 14(2):195–202, 1999. 2

[12] Bing L. Luk, David S. Cooke, Stuart Galt, Arthur A. Collie, and Sheng Chen. Intelligent legged climbing service robot for remote maintenance applications in hazardous environments. *Robotics and Autonomous Systems*, 53(2):142–152, 2005. 1

[13] Vladimir Lumelsky and Alexander Stepanov. Dynamic path planning for a mobile automaton with limited information on the environment. *IEEE Transactions on Automatic Control*, 31(11):1058–1063, 1986. 2

[14] Giacomo Lunghi, Raul Marin, Mario Di Castro, Alessandro Masi, and Pedro J. Sanz. Multimodal human-robot interface for accessible remote robotic interventions in hazardous environments. *IEEE Access*, 7:127290–127319, 2019. 1

[15] Dominique Martinez, Lotfi Arhidi, Elodie Demondion, Jean-Baptiste Masson, and Philippe Lucas. Using insect electroantennogram sensors on autonomous robots for olfactory searches. *Journal of Visualized Experiments: JoVE*, 90: 51704, 2014. 2

[16] Kimberly N. McGuire, Guido CHE de Croon, and Karl Tuyls. A comparative study of bug algorithms for robot navigation. *Robotics and Autonomous Systems*, 121:103261, 2019. 2

[17] Kimberly N. McGuire, Christophe De Wagter, Karl Tuyls, Hilbert J. Kappen, and Guido C. H. E. De Croon. Minimal navigation solution for a swarm of tiny flying robots to explore an unknown environment. *Science Robotics*, 4(35), 2019. 1, 2, 7, 8

[18] Saqib Mehmood, Shakeel Ahmed, Anders Schmidt Kristensen, and Dewan Ahsan. Multi criteria decision analysis (MCDA) of unmanned aerial vehicles (UAVs) as a part of standard response to emergencies. In *4th International Conference on Green Computing and Engineering Technologies*, page 31, 2018. 1

[19] Luis Merino, Fernando Caballero, J. Ramiro Martinez-de Dios, and Aníbal Ollero. Cooperative fire detection using unmanned aerial vehicles. In *2005 IEEE International Conference on Robotics and Automation*, pages 1884–1889, 2005. 1

[20] Andrew J. Myrick, Kye Chung Park, John R. Hetling, and Thomas C. Baker. Real-time odor discrimination using a bioelectronic sensor array based on the insect electroantennogram. *Bioinspiration & Biomimetics*, 3(4):046006, 2008. 2

[21] Eliyahu Osherovich, Vladimir Yanovki, Israel A. Wagner, and Alfred M. Bruckstein. Robust and efficient covering of unknown continuous domains with simple, ant-like a(ge)nts. *The International Journal of Robotics Research*, 27(7):815–831, 2008. 2

[22] Giovanni Pau, Fabio Arena, Yonas Engida Gebremariam, and Ilsun You. Bluetooth 5.1: An analysis of direction finding capability for high-precision location services. *Sensors*, 21(11):3589, 2021. 2, 7

[23] Samuel T. Pfister, Stergios I. Roumeliotis, and Joel W. Burdick. Weighted line fitting algorithms for mobile robot map building and efficient data representation. In *2003 IEEE International Conference on Robotics and Automation*, pages 1304–1311, 2003. 7

[24] Mateusz Przybyła. Detection and tracking of 2d geometric obstacles from LRF data. In *2017 11th International Workshop on Robot Motion and Control*, pages 135–141, 2017. 7

[25] Bijan Ranjbar-Sahraei, Gerhard Weiss, and Ali Nakisaee. A multi-robot coverage approach based on stigmergic communication. In *Multiagent System Technologies*, pages 126–138. Springer Berlin Heidelberg, 2012. 1, 2

[26] William Roberts, Kelly Griendling, Anthony Gray, and Dimitri N Mavris. Unmanned vehicle collaboration research environment for maritime search and rescue. *30th Congress of the International Council of the Aeronautical Sciences*, pages 1–5, 2016. 1

[27] Yuhui Shi and Russell Eberhart. A modified particle swarm optimizer. In *Evolutionary Computation Proceedings*, pages 69–73, 1998. 1

[28] Yoonchang Sung. *Multi-Robot Coordination for Hazardous Environmental Monitoring*. PhD thesis, Virginia Tech, 2019. 1

[29] Jonas Svennebring and Sven Koenig. Building terrain-covering ant robots: A feasibility study. *Autonomous Robots*, 16(3):313–332, 2004. 1

[30] Sebastian Thrun, Dieter Fox, Wolfram Burgard, and Frank Dellaert. Robust Monte Carlo localization for mobile robots. *Artificial Intelligence*, 128(1-2):99–141, 2001. 1

[31] Gábor Vásárhelyi, Cs Virágh, Gergo Somorjai, Norbert Tarcai, Tamás Szörényi, Tamás Nepusz, and Tamás Vicsek. Outdoor flocking and formation flight with autonomous aerial robots. In *2014 IEEE/RSJ International Conference on Intelligent Robots and Systems*, pages 3866–3873, 2014. 1

[32] Israel A. Wagner, Michael Lindenbaum, and Alfred M. Bruckstein. Distributed covering by ant-robots using evaporating traces. *IEEE Transactions on Robotics and Automation*, 15(5):918–933, 2002. 1

[33] Ouarda Zedadra, Hamid Seridi, Nicolas Jouandeau, and Giancarlo Fortino. S-MASA: A stigmergy based algorithm for multi-target search. In *2014 Federated Conference on Computer Science and Information Systems*, pages 1477–1485, 2014. 2

[34] Vittorio A. Ziparo, Alexander Kleiner, Bernhard Nebel, and Daniele Nardi. RFID-based exploration for large robot teams. In *2007 IEEE International Conference on Robotics and Automation*, pages 4606–4613, 2007. 1